T-TraCS – An automated method to measure soiling losses at parabolic trough receiver tubes

Cite as: AIP Conference Proceedings **2303**, 210006 (2020); https://doi.org/10.1063/5.0029685
Published Online: 11 December 2020

Fabian Wolfertstetter, Stefan Wilbert, Philipp Bellmann, Sergio Gonzales Rodriguez, Tomas Reche Navarro, Lothar Keller, and Aranzazu Fernandez-Garcia

T-TraCS – an Automated Method to Measure Soiling Losses at Parabolic Trough Receiver Tubes

Fabian Wolfertstetter[1, a)], Stefan Wilbert[1], Philipp Bellmann[2], Sergio Gonzales Rodriguez[1], Tomas Reche Navarro[1], Lothar Keller[1] and Aranzazu Fernandez-Garcia[3]

[1] *German Aerospace Center (DLR), Ctra Senés km 4, 04200 Tabernas, Spain.*
[2]*Technical University of Dresden, Faculty of Electrical and Computer Engineering, Helmholtzstr. 18, 01069 Dresden, Germany*
[3]*CIEMAT- PSA, Ctra. Senés km. 4, P.O. Box 44, 04200, Tabernas, Spain*

[a)]Corresponding author: Fabian.wolfertstetter@dlr.de

Abstract. Soiling of the envelope tubes of parabolic trough collectors can significantly reduce their transmittance and hence the overall collector efficiency. There are only a few methods to quantify soiling losses at absorber tubes of parabolic trough collectors. The existing methods are either laboratory based and cannot be applied automatically or they are personnel intense because they can only be used manually inside of operational solar fields. In this work we present a novel device called T-TraCS capable of automatically measuring the transmission of a sample glass during outdoor exposure with the current solar spectrum and imitating the movement of operational parabolic trough collectors. It can be used in resource assessment campaigns in order to better estimate future soiling losses at the tube level or it can be set up inside a solar field in order to measure the tube soiling losses in real time for CSP plant operation. Scattering simulations are presented that correct the measurement raw values of the T-TraCS and a spectrophotometer for their differences to the optics of a receiver tube. The validation with these final measurements shows good agreement with the reference spectrophotometer with a R2 of 0.996. The T-TraCS is therefore capable of automatically determining the soiling induced transmission losses with high accuracy.

INTRODUCTION

The issue of soiling in Concentrated Solar Power (CSP) parabolic trough collectors (PTC) has been mostly discussed for the mirror surfaces. There are very few studies available that investigate the transmission of glass envelopes of the receiver tubes (heat collector element, HCE) of the collectors[1]. It is widely accepted that the influence on the optical collector efficiency caused by accumulated dust is higher at mirror surfaces than at HCE glass envelopes. Nevertheless, its contribution cannot be neglected if a complete picture of the effect of soiling on PTCs is the goal. The effects of different cleaning methods on the absorber tube performance has been analyzed previously [2] with soiling rates of 0.1 – 0.3 %/day observed at the investigated tubes. These measurements of transmission have been performed using the mini incus sensor[2]. The mini incus is applicable only in operational solar fields [3]. The device is limited to full scale HCEs in order to be able to perform the measurements and has the advantage to be applicable inside operating solar fields. The device uses LED light sources with 15 different wavelengths and photodiodes to measure the transmitted light at the other end of the absorber tube. The light passes the glass envelope twice before it can be detected and the acceptance angle is not given in the reference. For reasons of the optical setup it must be smaller than the actual acceptance angle measured between one point on the outside of the glass envelope to the edges of the black absorber tube inside the envelope. For a normal incidence on the collector and Schott PTR70 HCEs this acceptance half angle is 30°.

SolarPACES 2019
AIP Conf. Proc. 2303, 210006-1–210006-10; https://doi.org/10.1063/5.0029685
Published by AIP Publishing. 978-0-7354-4037-1/$30.00

Another previous study exposed glass samples side by side (same orientations and inclinations) to mirror samples at seven sites in the USA [4]. They measure and compare reflectance and transmission values and determine constant exponentials that derive the combined tube and mirror soiling losses from the easier accessible mirror cleanliness measurements according to $C_{tot} = C_{mir} * C_{tube} \approx (C_{mir})^a$, where C stands for cleanliness and the indices refer to total (*tot*), mirror (*mir*) and tube (*tube*). The exponentials *a* range between 1.62 and 1.79 for glass samples exposed at the given sites. Their study concludes proposing to use these conversion exponentials to derive tube soiling rates. There are several reasons that show that this assumption is rather inaccurate: First, the light has to pass the soiling layer only once in a tube as compared to twice in second surface glass mirrors, secondly, the acceptance angle at the HCE is much higher than that at the mirror level which causes a much lower loss ratio of scattered light for the tubes. Furthermore, in operating troughs, absorber tubes will not sit still facing one direction during their exposure, but tracked according to the solar position. The region of the tube that are irradiated by the concentrated light is oriented towards the collector and thus in opposite directions as the mirrors. Because soiling heavily depends on the tilt angle during exposure, a derivation of the HCE soiling from mirror soiling is not trivial.

In this study we present a novel device named Transmission Tracking Cleanliness Sensor (T-TraCS) for measurements of the transmission of a glass sample during exposure to the environment. First we will describe its design and the underlying concept that led to the selection of the design parameters. Then the data acquisition and data evaluation is described and validation measurements are presented.

DESIGN OF THE T-TRACS

The design goal was an automated device for the measurement of soiling-induced transmission losses at HCE glass envelope samples for application in resource assessment measurement campaigns with highest possible measurement accuracy. One of the key parameters to achieve representative soiling behaviors is the position of the sample during the exposure. The measurement accuracy is influenced by parameters such as the solar spectrum used in measurement and the optical framework, i.e. acceptance angle, incident angles and geometry. The considerations will be treated in the following sub-sections.

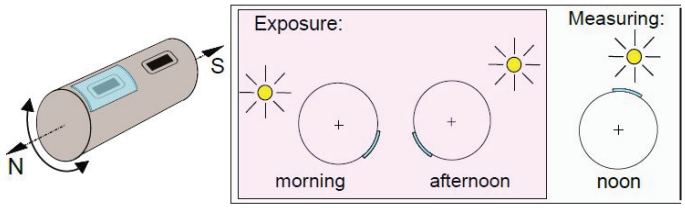

FIGURE 1. Illustration of the T-TraCS mounting orientation as well as exposure and measurement positions when looking towards the south. The measurement is sketched for a case closely after solar noon.

General Setup and Tracking Patterns

The aim of the T-TraCS is to expose the sample glass in the same way as the glass section on a HCE in operation that is transmitted by most of the concentrated radiation. Therefore, a stepper motor is included that rotates the tube around its axis. For an illustration of the exposure and measurement positions, see Fig. 1. The dimensions of the measurement device are the same as a typical tube used in actual power plants (PTR70). Therefore the general shape of the T-TraCS was chosen to be a 40 cm long aluminum tube with a diameter of 125 mm, see Fig. 2a). There are two apertures included in the tube below which pyranometers are located. One of the openings is covered by the glass sample to be measured, the other is covered by a flexible lid. The sample completely covers the pyranometer opening, avoiding any dust or dirt to settle on its sensitive surface. The sample is held by two metal arms that can be easily moved to exchange the sample. The lid above the other aperture is held in closed or open position by a spring connecting the lid and the tube. The force to close and open the lid is exerted by a metal string that engages in the hook while the tube rotates from measurement to exposure position or vice versa. For details of the lid's opening and closing mechanism, see Fig. 2b). The two pyranometers are mounted onto a metal plate that assures the correct alignment of the two instruments. There are two fans included at the lateral side of the tube that control the temperature inside the device with the help of a thermostat. The pyranometer mounting plate separates two sections inside the tube, assuring the ventilation of the entire tube volume.

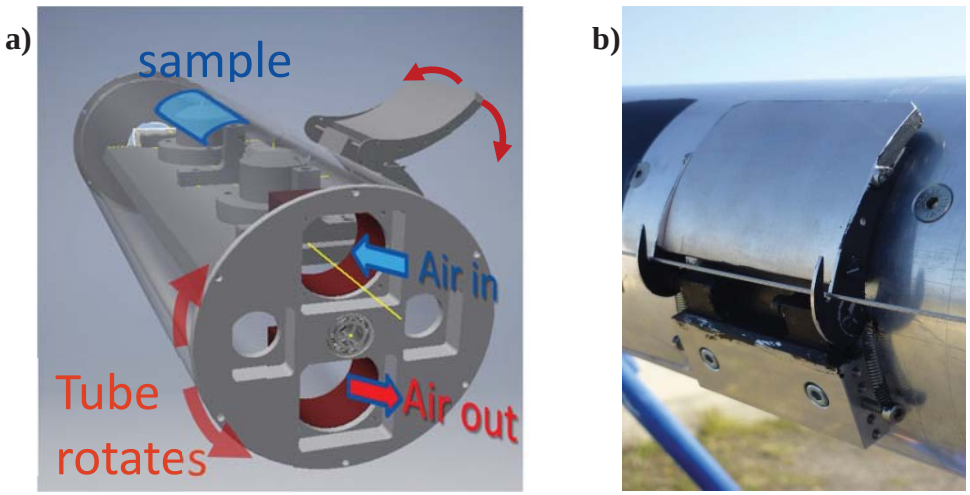

FIGURE 2. a) Technical drawing of the T-TraCS measurement device. The tube can be rotated around its axis, two openings for pyranometers are located co-planar; one of the openings is covered by the sample glass, the other by a flexible lid (**b**) that opens only for measurement and is closed the rest of the time to avoid soiling of the reference pyranometer.

During a measurement run, the pyranometer signals are logged together with the tube's rotational position. The measurement data acquisition begins at the time the flexible lid is opened passively and ends after passing the sun-facing direction by than 25°: The tube is then rotated backwards in order to go back to the exposure position. An example data set from one measurement run is shown in Fig. 3. The two pyranometer signals are shown as red and blue lines and the ratio of the two divided by the ratio for the clean sample is shown as the black line. The final cleanliness value for a measurement run is the average over a 10° window around the rotational position with maximum irradiance.

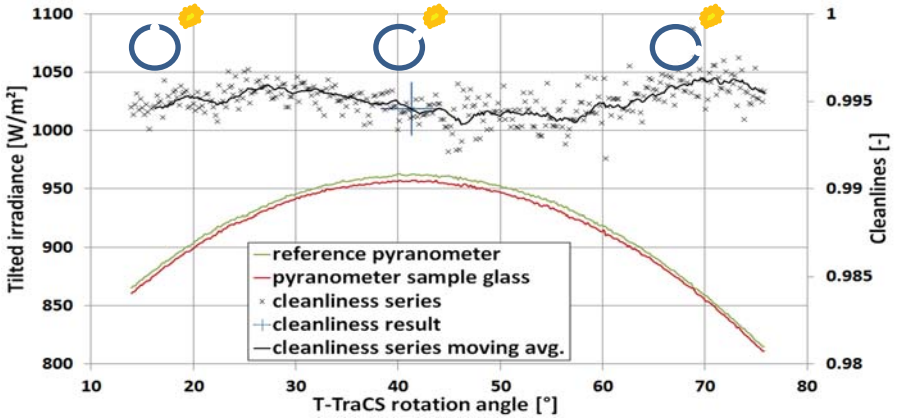

FIGURE 3. Data of an example measurement run. The average of the 10° interval around the maximum irradiance is determined as the cleanliness raw signal which is processed as described in the next sub-section. Each run delivers angle resolved transmission information. The rotational position of T-TraCS relative to the sun is indicated in the pictograms.

The T-TraCS setup has been installed at Plataforma Solar de Almeria (PSA) in May 2017. The setup is mounted on a height of 1.6 m above ground with the tube oriented in North-South direction. This is also the common direction for parabolic troughs located in similar latitudes as the PSA. The lower height as compared to the HCE in PTC plants was selected to enable a better comparison to mirror soiling.

DATA TREATMENT AND VALIDATION

In this section we want to summarize the derivation of the data correction applied during the data post processing of the T-TraCS device and the Perkin Elmer Spectrophotometer used as a reference in the validation measurement campaign. Transmission measurement setups for parabolic trough tubes should be comparable to the transmission in a real absorber tube in operation. As there are no automated optical measurement systems available that utilize a real absorber tube's geometrical setup, the assumptions are presented that allow for a comparison of transmission measurements taken with differing optics to the situation in a parabolic trough absorber tube, i.e. correction functions are developed that convert the transmission measurement signals to the actual losses experienced by the absorber tube.

The effect of soiling can be described by its reduction of optical efficiency compared to the clean absorber tube. If all other influences (coating efficiency, alignment, thermal conductivity, etc.) are held constant, the effect of soiling, quantified by the cleanliness, ξ, is the reduction of transmittance of the soiled absorber tube glass envelope (τ_{soiled}) compared to the transmittance of the clean one (τ_{clean}) following:

$$\xi = \frac{\tau_{soiled}}{\tau_{clean}}, \tag{1}$$

τ_{soiled} or τ_{clean} correspond to the ratio of the irradiance arriving at the receiver surface after passing the clean or soiled absorber glass (I_{glass}) to that hitting the absorber tube in the unobstructed case (I_0):

$$\tau = \frac{I_{glass}}{I_0}. \tag{2}$$

The transmitted irradiance can vary depending on the acceptance angle, the wavelength and the geometry used in the measurement setup. Figure 4 illustrates the geometries of the three setups relevant for this study, i.e. the T-TraCS instrument, the Perkin Elmer spectrophotometer used as the reference device in the validation measurement campaign and the HCE absorber tube as the case of application.

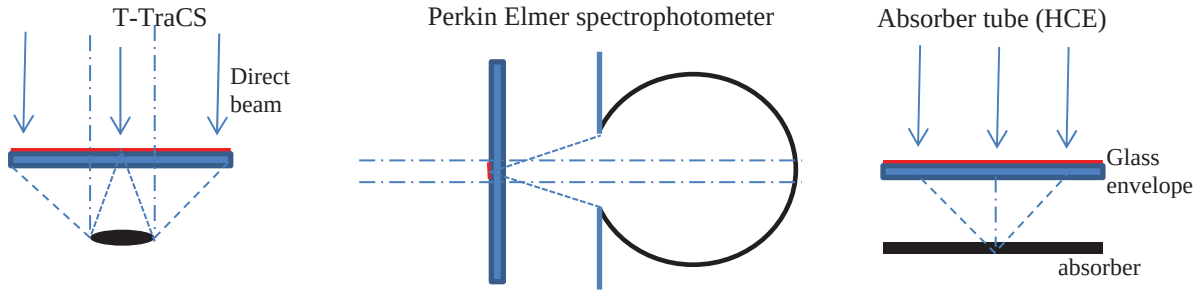

FIGURE 4. Optical situation in both measurement devices used for the validation measurement campaign and in the parabolic trough collector. Illuminated surface sections are shown in red, incident light rays are indicated as arrows, scattered rays are shown as dashed lines, transmitted rays as dash-dotted lines and detector (or absorber) surfaces in black.

Figure 5 a) shows the dimensions of a typical parabolic trough absorber tube in longitudinal cross section with the soiled and illuminated surface indicated in red. The red side faces the mirrors of the CSP collector that concentrates incident solar irradiance towards the absorber tube. The soiling effect on the irradiance contribution entering the opposite side of the tube, i.e. coming directly from the sun, is neglected as it only constitutes a share of 1/(concentration factor) ≈ 1/80 for a Eurotrough collector.

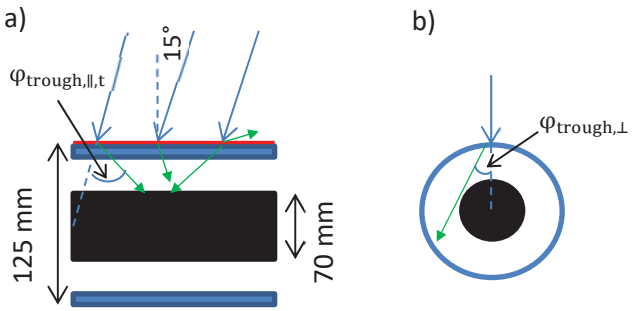

FIGURE 5. a) Longitudinal cross section of a parabolic trough tube and indication of the illuminated surface in red. Some example scattered rays are indicated in green. **b)** HCE tube cross section to illustrate the acceptance angle considerations for a normal incident ray that is scattered such to just miss the absorber tube. For the selected HCE the acceptance half angle is 29.2°.

The transmittance of the soiled tube is influenced by scattering and absorption effects of the dust. However, our scattering simulations presented below have shown that around 95% of the soiling losses can be attributed to scattering and only 5% to absorption at dust particles. In the following we will estimate the acceptance efficiency of the absorber tube as the ratio of radiation initially incident towards the receiver tube to the accepted radiation after scattering. Thereby we assume that all soiling losses are due to scattering. This is a simplification justified by the fact that absorption only accounts for 5% of the lost irradiance.

In the following we imagine a ray incident with 15° respective the normal on the tube axis. If no transversal scattering but only longitudinal scattering is present, scattered light reaches the receiver below the glass envelope if deviated by angles of up to 105° and 75° in longitudinal direction. Also see Fig 5 a). For the full acceptance angle ($\varphi_{trough,\parallel,t} + \varphi_{trough,\parallel,a}$) in longitudinal direction, the following equation holds for all incidence angles:

$$\varphi_{trough,\parallel,t} + \varphi_{trough,\parallel,a} < 2 \cdot 90°, \tag{3}$$

where the subscripts indicate if the angle is measured in the direction of the tube end showing more towards (*t*) the light source or away (*a*) from it. The difference between $\varphi_{trough,\parallel,t}$ and $\varphi_{trough,\parallel,a}$ will vary depending on the incidence angle.

In a parabolic trough absorber tube, the limit half acceptance angle in purely transversal direction of a ray hitting the center of the envelope tube in normal direction can be determined from the geometry shown in Fig. 5 b):

$$\varphi_{trough,\perp} = \operatorname{atan}\left(\frac{35\text{mm}}{62.5\text{mm}}\right) = 29.2°. \tag{4}$$

Increasing the incidence angle, $\varphi_{trough,\perp}$ will decrease. If the point of incidence on the tube is moved along the circumference of the tube asymmetric half acceptance angles are found. A similar expression as for longitudinal scattering can be found for normal incidence light

$$\varphi_{trough,\perp,t} + \varphi_{trough,\perp,a} \leq 2 * 29.2°, \tag{5}$$

where the indices indicate if the angle is meant towards the tube center (*t*) or away from it (*a*).

A full description of the acceptance angle distributions is not in the scope of this work, but the limit acceptance angles for the case of 15° incident light are shown in **TABLE 1** because during the validation measurements with the T-TraCS and the Perkin Elmer spectrophotometer, the same incidence angle is used in all instruments.

In the next step the optical setups of the measurement instruments employed in the validation campaign as shown in Fig. 4 are compared to that of the parabolic trough absorber tube. Then correction functions for the measurement instruments are developed in order to make the measurements as representative as possible of the effect of soiling on actual absorber tubes.

TABLE 1. transversal and longitudinal absorber tube acceptance angles for the case of 15° incidence light

Parameter	Value
$\varphi_{trough,\perp,t,15°} + \varphi_{trough,\perp,a,15°}$	$\leq 2 * 28.6°$
$\varphi_{trough,\parallel,t}$	105°
$\varphi_{trough,\parallel,a}$	75°

Spectrophotometer Correction Function

The acceptance angle of the Perkin Elmer spectrophotometer can be derived from the geometry of the illuminated surface on the glass sample, the radius of the aperture of the integrating sphere (12 mm) and the distance between the sample glass and the plane of the aperture (~45 mm). The half acceptance angle ($\varphi_{\mathrm{Perkin}}$) for the Perkin Elmer spectrophotometer for the measurement spot in the center of the illuminated surface is

$$\varphi_{\mathrm{Perkin}} = \operatorname{atan}\left(\frac{12\ \mathrm{mm}}{45\ \mathrm{mm}}\right) = 14.9°. \tag{6}$$

We will work with this specific acceptance angle as an approximation of the spectrophotometer's angular acceptance. However, it should be mentioned, that the radiation is partly accepted by the Perkin Elmer for an angular interval around the acceptance angle. This anglular interval is defined by the corners of the illuminated beam profile (see Fig. 6a) and the opposite and the coincident edge of the circular aperture (see Fig. 6b). These angles are calculated as

$$\varphi_{\mathrm{Perkin,min}} = \operatorname{atan}\left(\frac{12\ \mathrm{mm} - \sqrt{(4\ \mathrm{mm})^2 + (8\ \mathrm{mm})^2}}{45\ \mathrm{mm}}\right) = 3.9° \text{ and} \tag{7}$$

$$\varphi_{\mathrm{Perkin,max}} = \operatorname{atan}\left(\frac{12\ \mathrm{mm} + \sqrt{(4\ \mathrm{mm})^2 + (8\ \mathrm{mm})^2}}{45\ \mathrm{mm}}\right) = 25.0° \tag{8}$$

a)

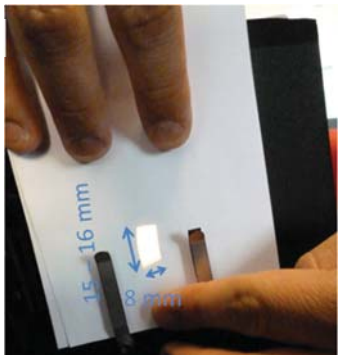

Perkin Elmer incident radiation cross section at the sample glass

b)

Perkin Elmer integrating sphere aperture

FIGURE 6. Pictures and dimensions of the Perkin Elmer optical framework: the light ray's cross section is smaller than the integrating sphere opening.

In order to correct the Perkin Elmer measurement to better fit the behavior of a receiver tube, the portion of the radiation being scattered in between 14.9° and 28.6° relative to the total scattered irradiance outside the 14.9° acceptance range has been estimated with a Mie based scattering simulation tool developed at DLR. The scattering tool delivers scattering phase functions for one particle diameter and wavelength as the one shown in Fig. 7. The phase functions over the 14.9° – 180° range are averaged and weighted with the particle scattering cross section, their size distribution number and the solar spectrum. The ratio of the corresponding average over the 14.9°- 28.6° range and that for the 14.9° to 180° range describes the radiation not detected by the Perkin Elmer but intercepted by the receiver. This ratio can be calculated as

$$C_{\mathrm{PE}} = \frac{\int_{14.9°}^{28.6°} \mathrm{P}(\varphi)\mathrm{d}\varphi}{\int_{14.9°}^{180°} \mathrm{P}(\varphi)\mathrm{d}\varphi} = 0.36, \tag{9}$$

where P is the averaged phase function. In this step an approximation is performed that takes into account only the perpendicular scattering angle and not the parallel acceptance angle of the absorber tube. This approximation is

sufficient to compare the two measurement instruments. The true correction factor to apply the measurements to a real tube would be somewhat greater than the one given above. The calculations were performed for mineral dust particles. There is a good agreement in literature for the index of refraction for mineral dust particles[5-7]. The value of $1.56 + 0.002i$ was used in this study. The particle size distribution as determined using microscopic measurements on soiled mirror surfaces in [8] is used and the phase function is averaged for this distribution. The particles are assumed to be spherical and only one particle-photon interaction is allowed per photon. A plot of the logarithm of the scattering phase function as determined with the Mie Plot algorithm for the given size distribution and refractive index and solar spectrum is shown in Fig. 7.

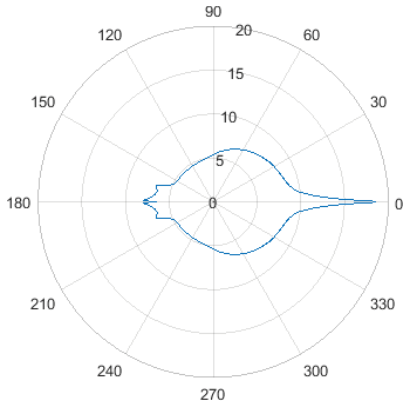

FIGURE 7. Logarithm of a scattering phase function plotted in radial direction against the scattering angle in polar direction. The particle sits in the middle of the graph and solar radiation hits the particles from the left, i.e. from 180°.

The scattered irradiance in the region outside the sensitive aperture of the Perkin Elmer, but inside the acceptance angle range of the absorber tube would contribute to the heat conversion in the tube and has to be added to the irradiance measured with the Perkin Elmer. The corrected irradiance that would be detected with a Spectrophotometer with an acceptance angle of 28.6° half acceptance angle can be approximated as

$$\mathrm{I_{PE,corr}} \approx \mathrm{I_{raw}} + (\mathrm{I_0} - \mathrm{I_{raw}}) * \int_{14.9}^{28.6} P(\varphi)\,\mathrm{d}\varphi = \mathrm{I_{raw}} + (\mathrm{I_0} - \mathrm{I_{raw}}) * \mathrm{C}_{PE} \tag{10}$$

where I stands for irradiance and the index *raw* means the irradiance measured with the acceptance angle of 14.9° as used in the Perkin Elmer Spectrophotometer. P is the normalized phase function as shown in Fig. 7.

Using the definition of the transmittance from above, the corrected transmission of the Perkin Elmer instrument can be derived as

$$\tau_{\mathrm{Perkin,corr}} \approx \frac{\mathrm{I_{PE.corr}}}{\mathrm{I_0}} = \tau_{\mathrm{Perkin,raw}} + \left(1 - \frac{\mathrm{I_{raw}}}{\mathrm{I_0}}\right) * \mathrm{C_{PE}} = (1 - \mathrm{C_{PE}})\tau_{\mathrm{Perkin,raw}} + \mathrm{C_{PE}} \tag{11}$$

This correction is applied to the Perkin Elmer transmission measurements in the next chapters. Note that we do not correct the Perkin Elmer measurement to the non-spherical shape of the absorber tube and the corresponding different losses in longitudinal and transversal directions as this is not required for the validation of the T-TraCS.

T-TraCS Correction Function

In the T-TraCS instrument, the acceptance angles can be derived in a similar approach using the detector diameter radius of 15 mm, the distance between the surface of the glass sample of 10 mm and the dimensions of the opening above the pyranometers of $38 \cdot 19$ mm^2. The acceptance half angle for a light ray incident on a spot on the glass sample located above the center of the pyranometer sensitive surface can be calculated as

$$\varphi_{\mathrm{TT,center}} = \mathrm{atan}\left(\frac{7.5}{10}\right) = 36.9° \tag{12}$$

Where the index *TT* stands for T-TraCS and *center* indicates that this acceptance angle corresponds to a central ray in normal incidence on the glass. For the 15° incidence angle as is the case in the experimental validation campaign

an adjusted acceptance angle is used: $\varphi_{TT,15} = 37.8°$. The angular interval for which radiation is accepted by the T-TraCS can be derived when moving the point of incidence on the glass surface laterally over the pyranometer's sensitive surface (diffusor). With similar considerations as for the Perkin Elmer, the acceptance interval of [0°, 56.3°]. is found. This range is thus bigger than that of the receiver tube in perpendicular direction. However, we continue to use the acceptance angle as an approximation.

The first step of the correction for the T-TraCS is calculated in analogy to the considerations above for the Perkin Elmer to deliver a correction function for the T-TraCS. The value for the correction factor C_{TT} is calculated as the irradiance scattered between 37.8° and 28.6° relative to the irradiance being scattered within the range >28.6°, resulting in $\mathbf{C_{TT} = 0.16}$. As the portion of the irradiance being measured with the T-TraCS is not relevant in the instrument comparison, it has to be subtracted in order to correct the raw measurement value from the T-TraCS:

$$I_{TT,corr,prelim} \approx I_{raw} - (I_0 - I_{raw}) * C_{TT}, \tag{13}$$

Therefore we find

$$\tau_{TT,corr,prelim} \approx \frac{I_{TT.corr,prelim}}{I_0} = \tau_{TT,raw} - \left(1 - \tau_{TT,raw}\right) * C_{TT}. \tag{14}$$

Additionally to the considerations regarding the acceptance angles the effect of positive contribution by scattered radiation from regions of the sample that would have normally not hit the pyranometer surface has to be taken into account. The effect can be explained when looking at the sketch of the T-TraCS optics on the left side of Fig. 4: the positively contributing irradiance trajectories are the two dashed lines that originate below the outermost incident rays. In the case without a glass (or with a perfectly clean glass) these rays would have not been registered by the pyranometer. This irradiance contribution has to be subtracted from the T-TraCS measurement raw value as this radiation would not contribute in the case of the corrected Perkin Elmer measurement.

In order to estimate the portion of radiation that contributes to the T-TraCS measurement and not the corrected Perkin Elmer signal, a sketch of the sample surface with the projection of the pyranometer sensitive surface on the glass sample is shown in Fig. 8a). The diameter of the diffusor of the pyranometer used in the T-TraCS is 15 mm. To best estimate the irradiance that positively influences the measurements, the scattering of radiation towards the pyranometer has to be calculated. Therefore we integrate the phase function from the smallest scattering angle from which a positive contribution originates until the largest contributing angle. The angles are calculated from the edge of the glass sample to the pyranometer sensitive surface. We obtain the range $\operatorname{atan}\left(\frac{7.5}{15}\right) = 26.5°$ to $\operatorname{atan}\left(\frac{30}{15}\right) = 63.4°$. Then this range is scaled by the total irradiance scattered outside 26.5°, estimated by all radiation scattered outside the T-TraCS acceptance angle of 37.8°.

This calculation delivers the positive scattering correction factor $\mathbf{C_{TT,pos} = 0.9}$. The surface area of the intersection of the plane of the pyranometer and the cone between 26.5° and 63.4° can be calculated as ~2200 mm^2. The area of the pyranometer sensitive surface is 176 mm^2, therefore a factor of 1/14 is introduced, as the pyranometer will only receive that fraction of the total scattered light in that angular range. In other words, the irradiance scattered in the angular range [26.5° 63.4°] is indicated in Fig. 8b) as the hoop in the plane of the pyranometer. Only the fraction of the total hoop surface that contains the pyranometer sensitive surface positively contributes to the irradiance measured by the pyranometer.

Furthermore, the area of the sample glass above the pyranometer opening is 722 mm^2 in area. The surface of the pyranometer sensitive surface is 176 mm^2 which fits 4 times into the former. Therefore, $C_{TT,pos}$ has to be multiplied by 4/14 in order to give the positive scattering contribution to the pyranometer measurement.

With these assumptions, the following correction function applies for cleanliness measurements taken with the T-TraCS instrument:

$$\tau_{TT,corr} \approx \frac{I_{TT.corr}}{I_0} = \tau_{TT,raw} - \left(1 - \tau_{TT,raw}\right) * C_{TT} - \left(1 - \tau_{TT,raw}\right) * C_{TT,pos} * 4/14 \tag{15}$$

The correction functions are applied to the raw data from measurements for the validation below. For the best comparison to the HCE effect, a more complex correction is possible. This correction is not presented here as it is not required for the validation with the Perkin Elmer.

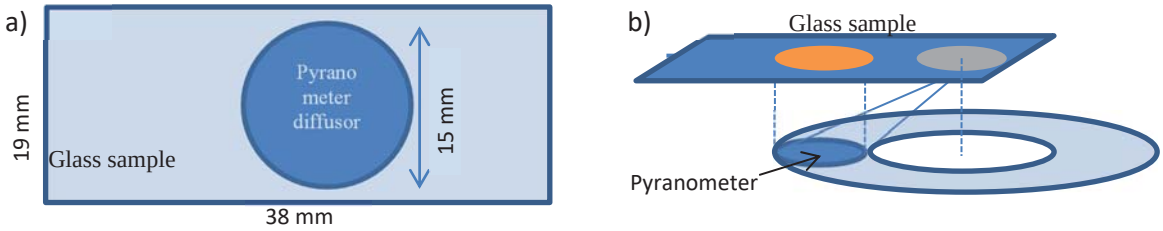

FIGURE 8. a) Sketch of the glass sample surface portion located above the T-TraCS opening used in the T-TraCS device for measurement of soiling. The projection of the measurement spot is shown. b) shows the projection of the measurement surface on the glass sample in orange

Results of the Validation Measurement Campaign

The validation measurement campaign has been performed using 12 glass samples that have been exposed in three phases to the natural environment at PSA. The samples are exposed in 4 different directions (north, east, south, west) and 3 different tilt angles (45°, 90°, 135°) plus one glass sample was exposed in horizontal tilt angle. Before the exposure, all samples have been measured with both devices to derive the clean transmission value. Then they were exposed for 4 weeks to the environment at a height above ground of approximately 1 m. After exposure they have been cleaned on the back side of the glass in order to avoid measurement of soiling that would not occur in a real parabolic trough absorber tube. Great care was taken not to affect the front side of the samples. Then they are measured with the Perkin Elmer spectrophotometer first and then with the T-TraCS device, both at a 15° incidence angle. In order to achieve a 15° incidence angle in the T-TraCS, it has been tilted towards the sun until the 15° angle was reached. A metal ruler with a 15° angle has been used to check the correct alignment of the T-TraCS towards the sun.

The spectrophotometer data is reported in spectral resolution of 10 nm step width. All spectral measurement data is weighted with the ASTM G173 standardized DNI solar spectrum for AM1.5 [9] and then converted to the cleanliness. Next, the correction function described in the previous sections is applied.

The T-TraCS measurements have been extracted from one measurement run each. After division by the individual transmission value of the clean sample, the correction as derived above is applied.

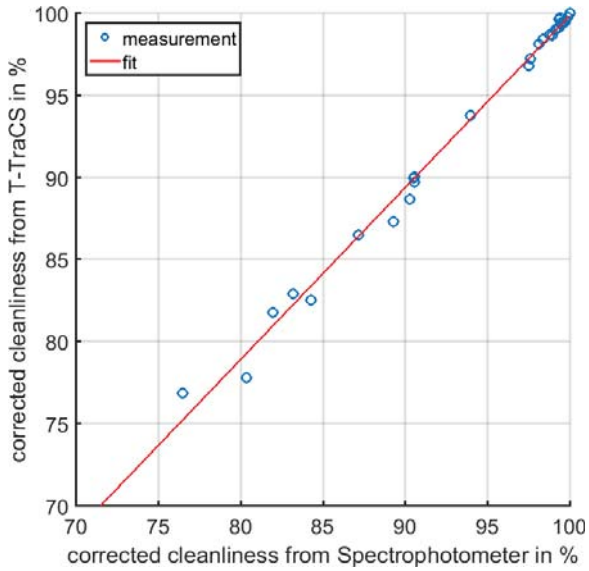

FIGURE 9. Validation measurement with naturally soiled glass samples that were measured with the Perkin Elmer and the T-TraCS devices.

The results of the validation measurement campaign are shown in Fig. 9. The corrected cleanliness measurements from both instrument show exceptional correlation to the fit curve with an R^2 of 0.996 and an RMSE of 0.6% cleanliness for the total range. The Perkin Elmer spectrophotometer's cleanliness is about 0.4 % higher on average than the T-TraCS measurement (bias). The reason for this is to be found in uncertainties in some of the assumptions included in the correction functions. It should be noted that the correction of the Perkin Elmers is stronger than the one for the T-TraCS and that the T-TraCS raw measurement is closer to the soiling effect in real HCEs, so that the validation is seen as successful despite of the small deviation. A validation campaign involving a full scale parabolic trough absorber tube might substantially lower these deviations, but the technical feasibility of such a measurement campaign is not given at the moment. The validation delivers similar results for all soiling levels down to 76%.

CONCLUSIONS

A novel automatic measurement device is presented for soiling measurements of absorber tube glass envelope samples during outdoor exposure. The device uses the solar irradiance as a radiation source and imitates the motion of an operational parabolic trough absorber tube during exposure. The instrument directly compares the irradiance measured by a pyranometer after transmission through a glass sample to that of an unobstructed pyranometer signal to derive the transmission of the sample. Comparison to the transmission with the clean glass gives the cleanliness of the sample.

Measurements are taken in regular intervals during rotation around its axis. In this way, incidence angle dependent transmission values can be derived.

Correction functions have been developed that involve scattering simulations in order to make the T-TraCS measurements more comparable to the situation in an operational trough. For the validation campaign, similar correction functions have been developed for the employed spectrophotometer. After correction, the cleanliness for both instruments agrees within a narrow error range.

ACKNOWLEDGEMENTS

This project has received funding from the European Union's Horizon 2020 research and innovation program under grant agreement No. 654479 (WASCOP).

REFERENCES

1. J. N. Hermoso and N. M. Sanz, Energy Procedia **69**, 1529-1539 (2015).
2. G. Espinosa-Rueda, N. Martinez-Sanz, D. Izquierdo-Nuñez and M. Osta-Lombardo, Journal of Solar Energy Engineering **138** (6), 061003 (2016).
3. G. Espinosa-Rueda, J. L. N. Hermoso, N. Martínez-Sanz and M. Gallas-Torreira, Solar Energy **135**, 122-129 (2016).
4. D. M. Deffenbaugh, S. T. Green and S. J. Svedeman, Solar Energy **36** (2), 139-146 (1986).
5. A. Petzold, K. Rasp, B. Weinzierl, M. Esselborn, T. Hamburger, A. DÖRNBRACK, K. Kandler, L. Schütz, P. Knippertz and M. Fiebig, Tellus B: Chemical and Physical Meteorology **61** (1), 118-130 (2009).
6. A. Rocha-Lima, J. V. Martins, L. A. Remer, M. Todd, J. H. Marsham, S. Engelstaedter, C. L. Ryder, C. Cavazos-Guerra, P. Artaxo and P. Colarco, Atmospheric Chemistry and Physics **18** (2), 1023-1043 (2018).
7. R. Wagner, T. Ajtai, K. Kandler, K. Lieke, C. Linke, T. Müller, M. Schnaiter and M. Vragel, Atmospheric Chemistry and Physics **12** (5), 2491-2512 (2012).
8. E. Roth and A. Anaya, Journal of Solar Energy Engineering **102** (4), 248-256 (1980).
9. ASTM, (ASTM International, West Conshohocken, PA, 2006).